Theoretical and Experimental Study of Amplifier Linearization Based on Harmonic and Baseband Signal Injection Technique

Chun-Wah Fan and Kwok-Keung M. Cheng, *Member, IEEE*

***Abstract*—This paper presents a novel linearization scheme for RF amplifiers based on simultaneous harmonic and baseband signal injection. In this method, second-order frequency components generated by predistortion circuits are fed to the input of the main amplifier to mix with the fundamental signal for third-order intermodulation distortion (IMD) cancellation. A general and rigorous analytical formulation of baseband, harmonic, and the proposed injection techniques is presented, and from these derived expressions, the optimum conditions for IMD suppression are developed. The result also reveals the practical limitation of the proposed method subject to gain and phase error associated with the RF and baseband circuitry. For comparison purposes, an amplifying system is constructed for the experimental investigation of second-order signal injection approach. Both two-tone and digitally modulated waveforms are employed in these measurements.**

***Index Terms*—Amplifiers, baseband, harmonic, linearization.**

I. INTRODUCTION

RECENT exploration in wireless applications puts further stress on the utilization of spectral efficient modulation scheme so as to accommodate more traffic in a limited bandwidth. Digital modulation is usually achieved through pulse-shaping technique which results in a time-varying waveform envelope. When this signal is fed to the RF power amplifier, intermodulation distortion is generated which gives rise to interfering signals in adjacent channels. In addition, this same phenomenon causes in-band interference and increased bit error rate. Out-of-band emission is caused by the saturation and phase distortion in RF amplifiers. In recent years, there has been a big resurgence of interest in the design of ultralinear power amplifiers for digital communication applications. Various linearization techniques have been proposed such as feedforward [1] and predistortion [2] that offer different degrees of performance at the expense of circuit complexity. Moreover, predistortion may be divided into baseband and RF schemes. Baseband predistortion focuses on the shaping of the waveform prior to up-conversion by using a lookup table or digital signal processor (DSP). On the other hand, RF predistortion uses analog circuitry to generate a nonlinear transfer characteristic, which is the reverse of the amplifier's transfer characteristics in both magnitude and phase.

Manuscript received July 16, 2001; revised September 17, 2001. This work was supported by a grant from the Research Grants Council of the Hong Kong Special Administrative Region under Project CUHK 4210/00E).

The authors are with the Department of Electronic Engineering, The Chinese University of Hong Kong, Hong Kong (e-mail: kkcheng@ee.cuhk.edu.hk).

Publisher Item Identifier 10.1109/TMTT.2002.800441.

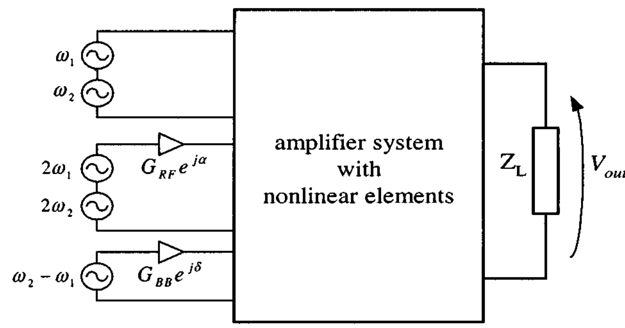

Fig. 1. General model of second-order signal injection system.

Recently, several methods based on the second-order signal injection have also been reported [3]–[6]. Intermodulation distortion (IMD) suppression is achieved by exploiting the second-order nonlinearity and second-order distortion signal at either the second-harmonic or baseband (difference) frequencies. Compared to the feedforward approach, this method tends to be simple and low cost. However, the second-harmonic approach requires both precise gain and phase adjustment for the perfect cancellation of the distorted signal, whereas the baseband method only gives limited IMD suppression (to be discussed in Section II).

This paper presents a new scheme for RF amplifier linearization based on simultaneous harmonic and baseband signal injection. This method is very stable, has no reduction in amplifier gain, and no need for precise phase adjustment. In Section II of this paper, the basic principle of second-order signal injection method is formulated by using the Volterra-series theory. Analysis shows the optimum conditions for the suppression of third-order intermodulation. In Section III, the effects of gain and phase error associated with the RF and baseband circuitry on the IMD suppression capability of the proposed method is addressed. Finally, the measured two-tone and vector signal test performances of an experimental amplifying system are shown for comparison.

II. METHOD OF ANALYSIS

Fig. 1 shows the general circuit model of the amplifying system under consideration. The amplifier is assumed to operate in the mildly nonlinear region in which the fifth- and higher order mixing products are negligibly small.

Active devices that are widely used in the design of RF amplifiers are FET and bipolar transistors. The circuit models of these devices may contain a number of parasitic components as well as nonlinear elements such as nonlinear gate-to-source capacitance, nonlinear base-to-emitter junction resistance, nonlinear drain current source, etc. In the Volterra-series analysis, the nonlinear characteristics of these elements are usually represented by a Taylor series expansion. For example, the nonlinear drain and gate current sources of a MESFET may be expressed as

$$i_{dsn}(t) = g_1 v_{gs}(t) + g_2 v_{gs}^2(t) + g_3 v_{gs}^3(t) \tag{1a}$$

$$i_{gsn}(t) = \frac{d}{dt}\left[C_1 v_{gs}(t) + C_2 v_{gs}^2(t) + C_3 v_{gs}^3(t)\right] \tag{1b}$$

where g_n and C_n ($n = 1, 2, 3$) are bias-dependent coefficients. To a first approximation, the Volterra series is truncated beyond the third-order term in the usual manner. Third-order mixing frequency component can be produced from the second-order (g_2 and C_2) and third-order (g_3 and C_3) nonlinearities. If the input source is assumed to consist of signal components at angular frequencies $\omega_1, \omega_2, 2\omega_1, 2\omega_2$ and $\omega_2 - \omega_1$, the output voltage at $2\omega_2 - \omega_1$ is, thus, given by

$$\begin{aligned} v_{\mathrm{out}}(2\omega_2 - \omega_1) &= \tfrac{3}{4}H_3(\omega_2, \omega_2, -\omega_1)\cdot v_s(\omega_2)\cdot v_s(\omega_2)\cdot v_s(-\omega_1) \\ &\quad + H_2(2\omega_2, -\omega_1)\cdot G_{\mathrm{RF}}\cdot e^{j\alpha}\cdot v_s(2\omega_2) \\ &\quad \cdot v_s(-\omega_1) + H_2(\omega_2-\omega_1, \omega_2)\cdot G_{\mathrm{BB}} \\ &\quad \cdot e^{j\delta}\cdot v_s(\omega_2-\omega_1)\cdot v_s(\omega_2) \end{aligned} \tag{2}$$

where $H_n(\,)$ is the nth order Volterra transfer function of the system [7]; G_{BB} and δ, G_{RF} and α are the voltage gain and phase shift associated with the baseband and RF paths, respectively. Note that the second-order signal interacts with the fundamental via the second-order nonlinearity of the amplifier to generate new components appearing at $2\omega_2 - \omega_1$. In fact, a predistortion circuit is used to produce these second-order signals from the original inputs at ω_1 and ω_2. Subsequently, these injection signals can be written as

$$v_s(2\omega_2) = \tfrac{1}{2}K_2(\omega_2, \omega_2)\cdot v_s(\omega_2)\cdot v_s(\omega_2) \tag{3}$$

$$v_s(\omega_2 - \omega_1) = K_2(\omega_2, -\omega_1)\cdot v_s(\omega_2)\cdot v_s(-\omega_1) \tag{4}$$

where $K_2(\,)$ denotes the second-order nonlinear transfer function of the predistortion circuit. Hence, the third-order IMD component may be expressed as

$$v_{\mathrm{out}}(2\omega_2 - \omega_1) = T_3(\omega_2, \omega_2, -\omega_1)\cdot v_s(\omega_2)\cdot v_s(\omega_2)\cdot v_s(-\omega_1)$$

where

$$\begin{aligned} T_3(\omega_2, \omega_2, -\omega_1) &= \tfrac{3}{4}H_3(\omega_2, \omega_2, -\omega_1) \\ &\quad + \tfrac{1}{2}G_{\mathrm{RF}}\cdot e^{j\alpha}\cdot H_2(2\omega_2, -\omega_1)\cdot K_2(\omega_2, \omega_2) \\ &\quad + G_{\mathrm{BB}}\cdot e^{j\delta}\cdot H_2(\omega_2-\omega_1, \omega_2)\cdot K_2(\omega_2, -\omega_1). \end{aligned} \tag{5}$$

Similarly, the third-order IMD signal at $\omega = 2\omega_1 - \omega_2$ is given by

$$v_{\mathrm{out}}(2\omega_1 - \omega_2) = T_3(\omega_1, \omega_1, -\omega_2)\cdot v_s(\omega_1)\cdot v_s(\omega_1)\cdot v_s(-\omega_2)$$

where

$$\begin{aligned} T_3(\omega_1, \omega_1, -\omega_2) &= \tfrac{3}{4}H_3(\omega_1, \omega_1, -\omega_2) \\ &\quad + \tfrac{1}{2}G_{\mathrm{RF}}\cdot e^{j\alpha}\cdot H_2(2\omega_1, -\omega_2)\cdot K_2(\omega_1, \omega_1) + G_{\mathrm{BB}} \\ &\quad \cdot e^{-j\delta}\cdot H_2(\omega_1-\omega_2, \omega_1)\cdot K_2(\omega_1, -\omega_2). \end{aligned} \tag{6}$$

By assuming that $\omega_2 \approx \omega_1$ and $\delta = 0$, (5) and (6) can be simplified as

$$\begin{aligned} r &= T_3(\omega_2, \omega_2, -\omega_1) \approx T_3(\omega_1, \omega_1, -\omega_2) \\ &= pe^{j\phi + j\Psi} + G_{\mathrm{RF}}\, de^{j\alpha + j\beta + j\Psi} + G_{\mathrm{BB}} qe^{j\Psi} \end{aligned}$$

where

$$\begin{aligned} &\tfrac{3}{4}H_3(\omega_2, \omega_2, -\omega_1) \\ &\quad \approx \tfrac{3}{4}H_3(\omega_1, \omega_1, -\omega_2) = pe^{j\phi + j\Psi} \\ &\tfrac{1}{2}H_2(2\omega_2, -\omega_1)\cdot K_2(\omega_2, \omega_2) \\ &\quad \approx \tfrac{1}{2}H_2(2\omega_1, -\omega_2)\cdot K_2(\omega_1, \omega_1) = de^{j\beta + j\Psi} \\ &H_2(\omega_2 - \omega_1, \omega_2)\cdot K_2(\omega_2, -\omega_1) \\ &\quad \approx H_2(\omega_1 - \omega_2, \omega_1)\cdot K_2(\omega_1, -\omega_2) = qe^{j\Psi}. \end{aligned}$$

Consequently, we have

$$|r|^2 = |pe^{j\phi} + G_{\mathrm{RF}}\, de^{j\theta} + G_{\mathrm{BB}} q|^2 \tag{7}$$

where $\theta = \alpha + \beta$. Inspection of (7) indicates that the distortion component ($pe^{j\phi}$) may be suppressed, with appropriate choices of the amplifier gains (G_{RF} and G_{BB}) and phase angle (θ). Related studies of second-order techniques using either the RF or difference-frequency injection have been reported elsewhere [3]–[6].

Case A: No Injection

In the absence of both baseband and RF injection ($G_{\mathrm{RF}} = G_{\mathrm{BB}} = 0$), (7) can be written as

$$|r| = p. \tag{8}$$

This IMD value is used as a reference level for comparison in the following cases.

Case B: Baseband Injection Only

From a practical point of view, it is simpler to use baseband rather than harmonic signal, which is at a substantially higher frequency. If we let $G_{\mathrm{RF}} = 0$, expression (7) becomes

$$\begin{aligned} |r|^2 &= |pe^{j\phi} + G_{\mathrm{BB}} q|^2 \\ &= (pc\cos\phi + G_{\mathrm{BB}} q)^2 + p^2 \sin^2\phi. \end{aligned} \tag{9}$$

The optimum condition for minimizing $|r|^2$ is

$$\frac{G_{\mathrm{BB}} q}{p} = -\cos\phi \tag{10}$$

and the corresponding IMD output can be evaluated by

$$\left|\frac{r}{p}\right|^2 = \sin^2\phi \tag{11}$$

where $|r/p|^2$ and $G_{\rm BB}q/p$ are, respectively, the IMD suppression factor and the normalized baseband signal gain required. These results suggest that only the in-phase component of the distortion signal may be eliminated and, hence, only partial cancellation of IMD is possible with the low-frequency injection approach. The amount of residual IMD ($\sin^2\phi$) depends on various parameters including the device's nonlinearities, parasitic components, and embedded circuit impedance levels. It is also clear from (7) that $G_{\rm BB}$ is real with either zero or 180° phase value and, therefore, only a constant gain amplifier is required to maintain low distortion output. In this approach, the phase shift associated with the low-frequency responses of the circuitry at $\omega = \omega_2 - \omega_1$ is the major limiting factor for broadband operation.

Case C: Harmonic Injection Only

The harmonic method may be obtained by setting $G_{\rm BB} = 0$ in (7), and the resulting expression for third-order intermodulation is given by

$$|r| = |pe^{j\phi} + G_{\rm RF}de^{j\theta}|.$$

For optimum cancellation of the distortion signal, the following conditions should be satisfied:

$$\frac{G_{\rm RF}d}{p} = 1 \tag{12}$$

$$\theta = \pi + \phi. \tag{13}$$

It can be shown that the gain $(G_{\rm RF})$ and phase (θ) of the RF path must be controlled to within a fraction of a decibel and a few degrees in order to attain maximum IMD reduction.

Case D: Harmonic and Baseband Injection

In the conventional harmonic injection method, the degree of achievable distortion cancellation is limited by the accuracy of the gain and phase shift introduced by the feeding networks. In the presence of both second-harmonic and baseband injection signals, it is possible to optimally suppress the third-order IMD by adjusting the gains of the amplifiers only, where θ becomes an arbitrary constant. And according to (7), we have

$$|r| = |pe^{j\phi} + G_{\rm RF}\,de^{j\theta} + G_{\rm BB}q| = 0$$

or

$$p\cos\phi + G_{\rm RF}\,d\cos\theta + G_{\rm BB}q = 0$$
$$p\sin\phi + G_{\rm RF}\,d\sin\theta = 0.$$

The optimum conditions for perfect IMD cancellation can, therefore, be derived as

$$\frac{G_{\rm BB}q}{p} = -\frac{\sin(\theta-\phi)}{\sin\theta} \tag{14}$$

$$\frac{G_{\rm RF}d}{p} = -\frac{\sin\phi}{\sin\theta}. \tag{15}$$

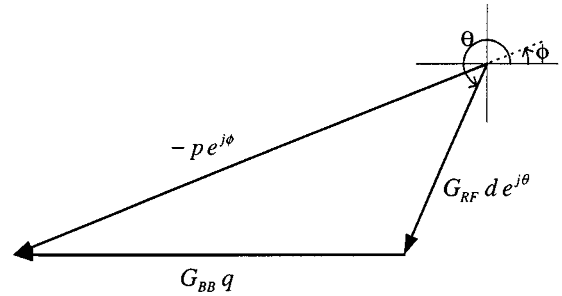

Fig. 2. Vector representation of (7).

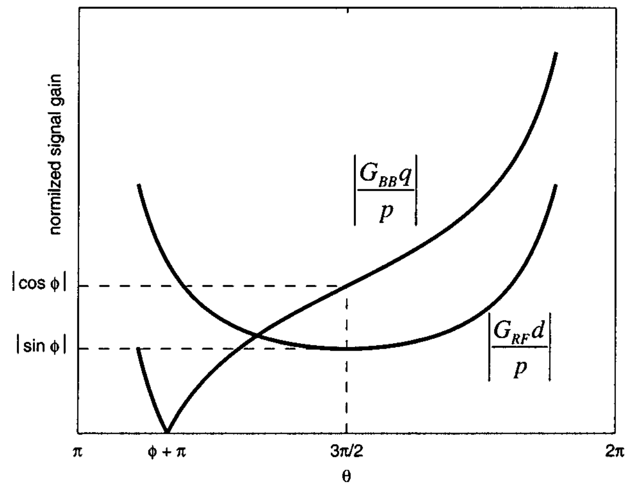

Fig. 3. Variation of normalized signal gain required as a function of θ.

The above expressions indicate that the distorted signal can be completely suppressed, provided that $\theta \neq 0$ and $\theta \neq \pi$. As depicted in Fig. 2, the combination of the two subvectors may be used to cancel out the distortion component $pe^{j\phi}$, by controlling the values of $G_{\rm BB}$ and $G_{\rm RF}$ at any arbitrary θ value (but phase reversal might be required). Fig. 3 shows the variation of the normalized signal gains $|G_{\rm BB}q/p|$ and $|G_{\rm RF}d/p|$ as a function of phase angle θ. In practice, if minimal RF signal gain is required, the two subvectors should be placed in phase quadrature ($\theta = 3\pi/2$). The corresponding values of $|G_{\rm BB}q/p|$ and $|G_{\rm RF}d/p|$ are simply equal to $|\cos\phi|$ and $|\sin\phi|$, respectively.

III. Effects of Gain and Phase Error

Some work has been done to see how sensitive this method is to changes in circuit parameters associated with the RF and baseband signal paths.

A. Effect of Gain Error

If the gain errors associated with the RF and baseband paths are denoted as $\Delta G_{\rm RF}$ and $\Delta G_{\rm BB}$, respectively, the corresponding output IMD signal may, therefore, be derived as

$$\begin{aligned}|r|^2 &= |pe^{j\phi} + (G_{\rm RF}+\Delta G_{\rm RF})\,de^{j\theta} \\ &\quad + (G_{\rm BB}+\Delta G_{\rm BB})q|^2 \\ &= |\Delta G_{\rm RF}\,de^{j\theta} + \Delta G_{\rm BB}q|^2 \\ &= (\Delta G_{\rm RF}\,d\sin\theta)^2 + (\Delta G_{\rm RF}\,d\cos\theta + \Delta G_{\rm BB}q)^2.\end{aligned}$$

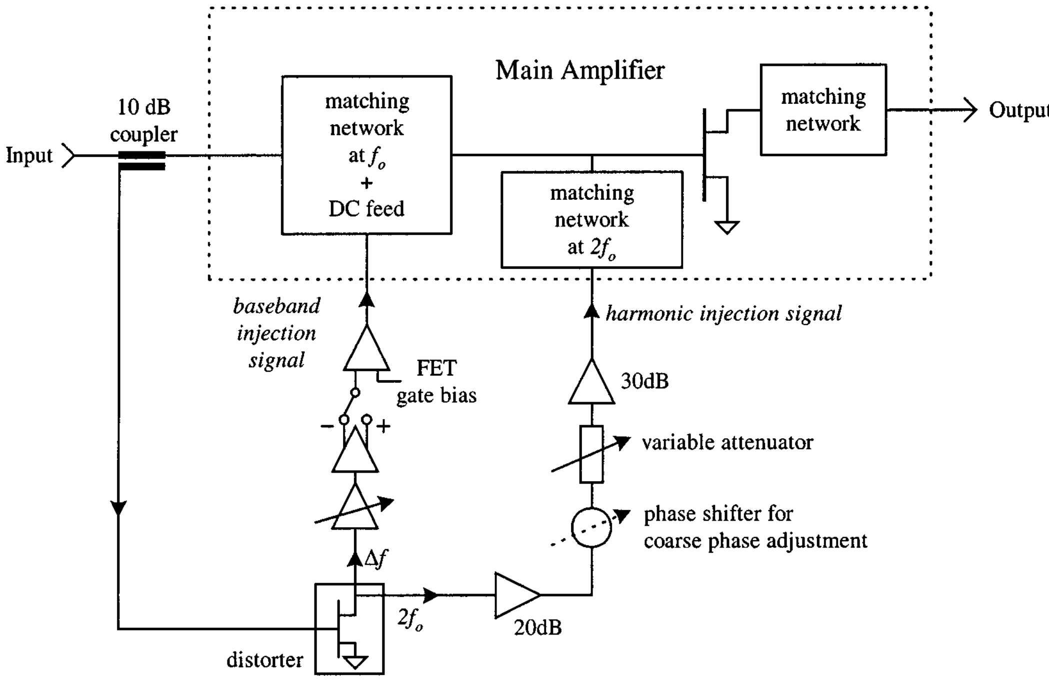

Fig. 4. Experimental setup.

In the worst case, the above expression can be written as

$$\left|\frac{r}{p}\right|^2 = \left(\frac{\Delta G_{\rm RF}\, d}{p}\right)^2 + \left(\frac{\Delta G_{\rm BB} q}{p}\right)^2 + 2\left|\frac{\Delta G_{\rm RF}\, d}{p}\right| \cdot \left|\frac{\Delta G_{\rm BB} q}{p}\right| \cdot |\cos\theta|. \quad (16)$$

Inspection of (16) indicates that the distortion signal is minimized by setting $\theta = 3\pi/2$, which leads to

$$\left|\frac{r}{p}\right|^2 = \left(\frac{\Delta G_{\rm RF}}{G_{\rm RF}}\right)^2 \cdot \left(\frac{G_{\rm RF} d}{p}\right)^2 + \left(\frac{\Delta G_{\rm BB}}{G_{\rm BB}}\right)^2 \cdot \left(\frac{G_{\rm BB} q}{p}\right)^2$$

$$\left|\frac{r}{p}\right|^2 = \left(\frac{\Delta G_{\rm RF}}{G_{\rm RF}}\right)^2 \sin^2\phi + \left(\frac{\Delta G_{\rm BB}}{G_{\rm BB}}\right)^2 \cos^2\phi.$$

Furthermore, it should be noted that, for the harmonic injection approach, the performance degradation due to gain mismatch is given by $|r/p|^2 = |\Delta G_{\rm RF}/G_{\rm RF}|^2$. In practice, $\sin^2\phi \ll 1$ and, therefore, the IMD performance of the proposed method is relatively less sensitive to the gain error of the RF path.

B. Effect of Low-Frequency Phase Shift

When the difference frequency becomes large under broadband operation, (5) and (6) indicate that the signal components at $\omega_1 - \omega_2$ and $\omega_2 - \omega_1$ are a complex conjugate pair. Because of this, the IMD signal at $2\omega_1 - \omega_2$ and $2\omega_2 - \omega_1$ cannot be totally suppressed by the proposed method. Mathematically, this effect can be modeled as

$$|r| = |pe^{j\phi} + G_{\rm RF}\, de^{j\theta} + G_{\rm BB} qe^{j\delta}|$$
$$\approx |pe^{j\phi} + G_{\rm RF}\, de^{j\theta} + G_{\rm BB} q(1 + j\delta)|$$
$$\left|\frac{r}{p}\right| = \left|\frac{G_{\rm BB} q}{p}\delta\right| = \left|\frac{\sin(\theta-\phi)}{\sin\theta}\right| \cdot |\delta|$$

where δ denotes the phase shift introduced by the low-frequency circuitry at $\omega = \omega_2 - \omega_1$, and for $\theta = 3\pi/2$, we have

$$\left|\frac{r}{p}\right|^2 = \cos^2\phi \cdot \delta^2. \quad (17)$$

If the baseband injection method is adopted instead, the residual IMD levels are then given by

$$\left|\frac{r}{p}\right|^2 \approx \sin^2\phi + \cos^2\phi \cdot \delta^2 - \sin 2\phi \cdot \delta, \qquad \text{for } \omega = 2\omega_2 - \omega_1 \quad (18)$$

$$\left|\frac{r}{p}\right|^2 \approx \sin^2\phi + \cos^2\phi \cdot \delta^2 + \sin 2\phi \cdot \delta, \qquad \text{for } \omega = 2\omega_1 - \omega_2. \quad (19)$$

The results shown in (17)–(19) suggest that the proposed method is more capable for broadband operation. In practice, the effect of δ may be minimized by using either a baseband amplifier with a large gain-bandwidth product or phase compensation network.

IV. Experiments and Discussions

The test setup for the IMD measurement is given in Fig. 4. The one-stage MESFET amplifier under test is a common-source configuration with input and output impedance matching networks. The transistor used is an Infineon Technologies CFY30. The main amplifier is designed to have two RF input ports: one for the fundamental and the other for the second-harmonic injection. High isolation between the two ports is achieved by using harmonic filters. Some filtering is also incorporated into the drain circuit to reduce the harmonic signal from reaching the output. Moreover, baseband signal is injected into the circuit through the gate-biasing network.

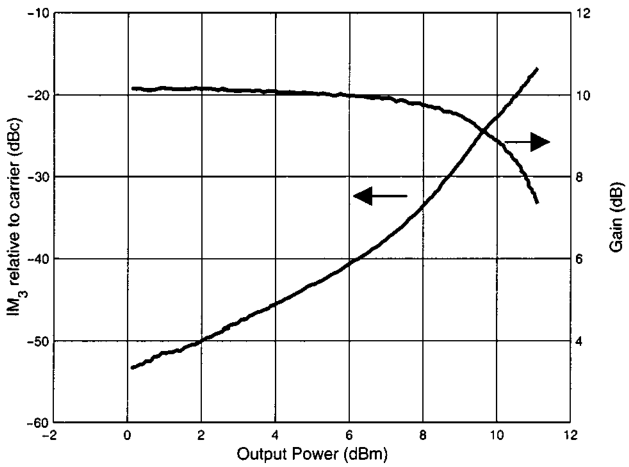

Fig. 5. Measured gain and IM_3 characteristics of the amplifier before linearization.

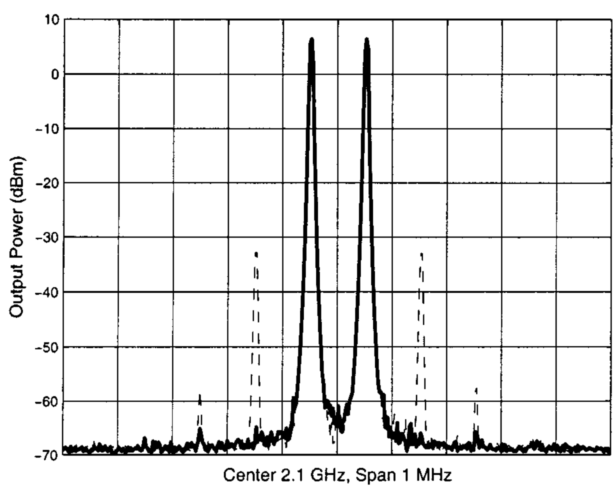

Fig. 6. Two-tone test of the amplifier (output power = 6.5 dBm).

The predistortion circuit is constructed using MESFET device, operating near pinchoff, for the generation of the second-order frequency components. The harmonic signal path consists of a preamplifier, a variable attenuator, and a high-gain amplifier. A variable phase shifter is inserted into the harmonic path for phase adjustment. The baseband circuit consists of a low-pass filter, a tunable gain amplifier, and an inverter. For the two-tone test, signals centered at about 2.1 GHz with a frequency spacing of 100 kHz are used. For the vector modulated signal measurement, 384-kb/s $\pi/4$ differential quadrature phase-shift keying (DQPSK) with random data is employed. Fig. 5 shows the plots of the measured third-order IMD and gain characteristics of the experimental amplifier, in the absence of any second-order signal injection. The module is found to exhibit a small-signal gain of about 10 dB and an output power of approximately 9.5 dBm at 1-dB gain compression point.

A. Two-Tone and Vector Signal Test Performance

The output frequency spectrum of the main amplifier, measured at an output power of 6.5 dBm, is shown in Fig. 6 for illustration. The gain levels of the RF and baseband paths are adjusted for minimum third-order IMD level. Improvement factor

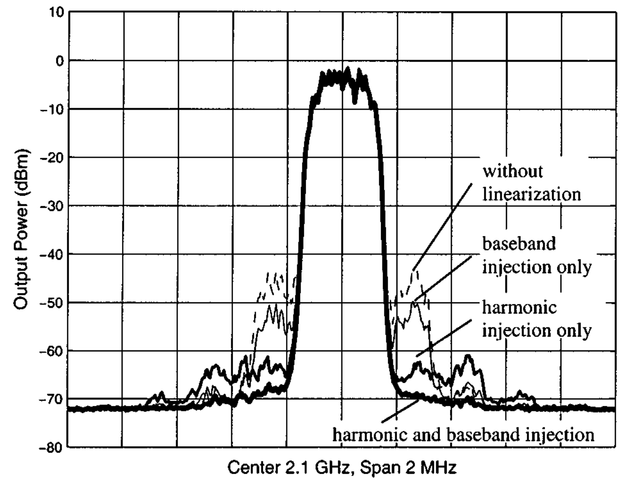

Fig. 7. Vector signal test of the amplifier (average output power = 11 dBm).

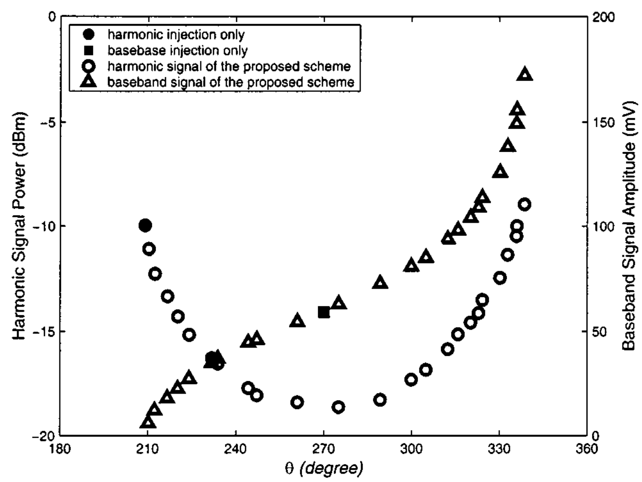

Fig. 8. Measured RF and baseband signal strength versus θ.

for the proposed scheme is about 30 dB and this value is limited by the noise floor of the measuring equipment and by the resolution of the variable attenuator used. Similar results were also observed for different θ values. In Fig. 7, the performance of the proposed technique, the baseband injection technique, and the harmonic injection technique are compared. It is clear that, for the proposed technique, a reduction factor of, respectively, 25 and 8 dB was achieved for the first and second side-lobe power levels. In contrast, the conventional baseband injection technique ($G_{\mathrm{RF}} = 0$) shows an IMD suppression factor of only 6 dB. Moreover, Fig. 8 shows the plot of the measured harmonic and baseband signal level required as a function of θ.

B. IMD Suppression Versus Output Power Level

In most linearization systems, adaptive control circuitry is usually required to maintain a low-distortion output as the input power level varies. Fig. 9 shows the measured third-order IMD level as a function of output power for the three injection methods under consideration. The performance of each scheme is optimized for minimum third-order IMD at an output power of 7.5 dBm. The results indicate that a substantial amount of IMD reduction (>20 dB) is achieved with the proposed method over a wide range of output power level. Note that

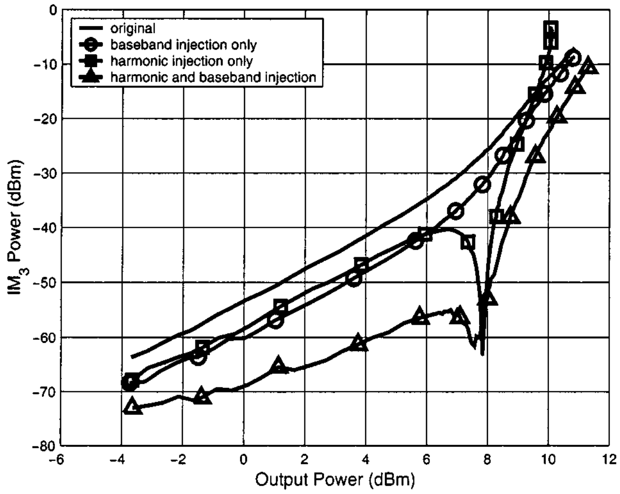

Fig. 9. Measured third-order IMD level as a function of output power.

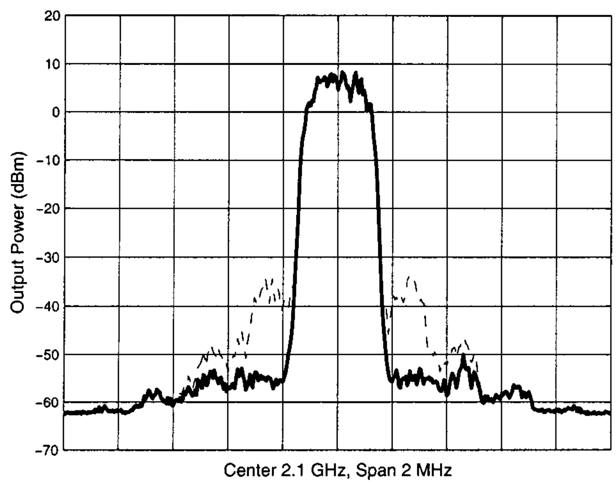

Fig. 10. Measured output spectrum of a medium-power amplifier (average output power = 21 dBm).

under small input signal condition, the IMD level is limited only by the dynamic range of the measuring equipment. It is also observed that the IMD performance deteriorates as the output power increases toward the 1-dB compression point. This phenomenon is believed to be due to the higher order mixing effect that has not been included above. Besides, for a strongly nonlinear case, reduction of the higher order IMD such as IM5 is indeed important [8].

Finally, Fig. 10 shows the measured output spectrum of another 2.1-GHz experimental amplifier module, operating at an average output power of 21 dBm. More than 20-dB suppression of IMD level is observed in this case. In principle, this technique can also be applied to high power devices as long as the amplifier is not operating too close to saturation.

V. Conclusions

A novel and effective approach to amplifier linearization by second-order signal injection has been described. Unlike the conventional second-harmonic injection method, no precise control of the amplitude and phase angle of the injected RF signal is required by the new scheme. The analysis also indicates that a 270° phase shift (θ) in the RF path is optimal for minimizing the effect of gain error on the IMD performance of the proposed method. Furthermore, it is shown experimentally that a large IMD reduction factor can be achieved with the proposed method over a wide output dynamic range.

References

[1] D. Myer, "Ultra linear/feedforward amplifier design," in *IEEE MTT-S Int. Microwave Symp. Dig.*, 1998, pp. 1125–1127.
[2] A. Katz, A. Guida, R. Dorval, and J. Dragone, "Input adaptive linearizer system," in *IEEE MTT-S Int. Microwave Symp. Dig.*, 2000, pp. 1499–1502.
[3] M. R. Mozzam and C. S. Aitchison, "A low third order intermodulation amplifier with harmonic feedback circuitry," in *IEEE MTT-S Int. Microwave Symp. Dig.*, 1996, pp. 827–830.
[4] D. Jing, W. S. Chan, S. M. Li, and C. W. Li, "New linearization method using interstage second harmonic enhancement," *IEEE Microwave Guided Wave Lett.*, vol. 8, pp. 402–404, Nov. 1998.
[5] Y. Hu, J. C. Mollier, and J. Obregon, "A new method of third-order intermodulation reduction in nonlinear microwave systems," *IEEE Trans. Microwave Theory Tech.*, vol. MTT-34, pp. 245–250, Feb. 1986.
[6] Y. Yang and B. Kim, "A new linear amplifier using low-frequency second-order intermodulation component feedforwarding," *IEEE Microwave Guided Wave Lett.*, vol. 9, pp. 419–421, Oct. 1999.
[7] J. J. Bussgang, L. Ehrman, and J. W. Graham, "Analysis of nonlinear systems with multiple inputs," *Proc. IEEE*, vol. 62, pp. 1088–1117, Aug. 1974.
[8] C. W. Fan and K. K. M. Cheng, "Reduction of third- and fifth-order IMD products in microwave amplifiers by the extended harmonic–baseband approach," , to be published.

Chun-Wah Fan received the B.Eng. and M.Phil. degrees in electronic engineering in 1996 and 1998, respectively, from The Chinese University of Hong Kong, Hong Kong, where he is currently working toward the Ph.D. degree.

His research interests include monolithic microwave integrated circuit (MMIC) design, amplifier linearization, RF and microwave nonlinear circuits, and device modeling.

Kwok-Keung M. Cheng (S'90–M'91) received the B.Sc. degree (with first-class honors) in electrical engineering and the Ph.D. degree from King's College, University of London, London, U.K., in 1987 and 1993, respectively.

In 1996, he became an Assistant Professor in the Department of Electronic Engineering, The Chinese University of Hong Kong, Hong Kong. He has authored or coauthored more than 35 papers published in leading international journals and conferences, and was a contributing author of *MMIC Design* (London, U.K.: IEE Press, 1995). His current research interests are concerned with the design of MMICs, oscillators, active filters, and power amplifiers.

Dr. Cheng was the recipient of the 1986 Siemens Prize, the 1987 Institution of Electrical Engineers Prize, and the 1988 Convocation Sesquicentennial Prize in Engineering (University of London).